PROCEEDINGS of the
23rd International Congress on Acoustics

9 to 13 September 2019 in Aachen, Germany

Aerofoil trailing edge self-noise reduction by Surface Mounted Attenuation Devices

Edvard SCHROEDER[1]; Tze Pei CHONG[1]; M. KAMRUZZAMAN[2]; Jeremy HURAULT[2]; Phillip JOSEPH[3]

[1]Department of Mechanical and Aerospace Engineering, Brunel University London Uxbridge, United Kingdom, UB8 3PH

[2]Vestas Technology UK Ltd, Newport, Isle of Wight, United Kingdom, PO30 5TR

[3]ISVR, University of Southampton, Southampton, United Kingdom, SO17 1BJ

ABSTRACT

This paper presents the results of a preliminary experimental study into the effect of add-on type finlets on the aeroacoustic performance of a wind turbine aerofoil. The content mainly deals with the turbulent boundary layer - trailing edge broadband noise characteristics subjected to the add-on finlets. The test program seeks to test various combinations of finlet height and spacing present on the (1) suction side only, (2) pressure side only, and (3) both suction and pressure sides. Each finlet parameter configuration is tested at jet velocity U=30m/s and 45m/s, at geometric angles of attack AOA (Angle of Attack) (geometric) = 10°, 0°, -10°. Based on the data acquired thus far it is observed that a finlet usually performs best with increasing height and decreasing spacing. Under configurations (1) and (2), finlets are able to produce up to 2dB Sound Power Level broadband noise reductions, where configuration (3) offers broadband reductions of up to 7dB Sound Power Level, with potential to observe more reductions once optimised. The main parameter for improved performance of finlets is the spacing rather than the height. Finlet height does not offer significant impact on the performance if the spacing is not optimal. The established trend for optimal finlet parameters remains consistent for all AOA, offering improved performance at high positive angles, which has a practical application to wind turbine blades.

Keywords: finlets, trailing edge, aerofoil, noise, reduction

1. INTRODUCTION

The current GEN1 STE (Serrated Trailing Edge) technology enabled wind turbine manufacturers to reduce the turbine self-noise predominantly in the range of 5-7dB in lab conditions (Gruber, Joseph, & Chong, 2010) (Moreau, Brooks, & Doolan, 2011) and validated to reduce in the range of 1.5-3dB in various field tests (Mathew, Singh, Madsen, & Leon, 2016). Now, in a wider scope, noise regulations on peri-urban areas place a strict clamp on noise emissions emitted from various aspects of the specified environment, be it residential, transport, infrastructural, or industrial. The wind industry is faced with a decision to meet these strict environmental regulations, either make the turbines quieter, or run them slower. It is evident that de-rating a wind turbine for several hours a day, over the span of a year add up to an immense quantity of lost kilowatt-hours in AEP (Annual Energy Production), and therefore a loss in profit. STEs have enabled turbines to run faster, and for longer under conditions where they would normally have to be de-rated. This results in a 6% AEP increase per turbine (Van Der Velden, Romani, & D.Casalino, 2018).

In a mission to further reduce noise emissions from wind turbines, enabling them to be placed either closer to populated areas, or operate at higher RPMs (Revolutions Per Minute) under noise emission restrictions, new types of passive devices must be considered beyond current STE technology. The nominal target is to achieve a further 3dBA noise reduction across a grouping of turbines.

TBL - TE (Turbulent Boundary Layer – Trailing Edge) noise accounts for most of the noise emission in wind turbine blades operating within their design regimes. As described in the previous section, the components of this mechanism include a turbulent boundary layer, resultant fluctuations in flow pressure, and a surface to scatter from, namely the trailing edge. To introduce changes into this mechanism, altering any one of these components will result in the spectral noise characteristics of the subject aerofoil.

A device/technique of particular interest comes from research done by (Millican, 2017) and (Clark, et al., 2015) from Virginia Polytechnic Institute which describes how the thick follicles on the trailing

edge of an owl's wing create a sort of canopy, and thus suppress any pressure fluctuations. The parameters at play are the finlet spacing, height, and extension beyond the trailing edge. Firstly, the trailing edge extensions are detrimental to noise reduction performance, so will not be included as a parameter in the testing. The height parameter increases the performance of the finlet, especially at high AOAs (Clark, et al., 2015). The final parameter is the finlet spacing, where a smaller gap will continue to improve the noise reduction performance to the point where they are small enough to cause vortex shedding. Noise reductions attained to date are in the region of 2-7dB SPL (Sound Pressure Level) from 1.5 to 10kHz (Millican, 2017). An emerging hypothesis suggests that the finlet performance is mainly accredited to the sheltering of the trailing edge from large turbulence structures, and the reduction of spanwise coherence of these structures.

A detailed study done by (Afshari, Szoke, Denghan, & Azarpeyvand, 2016) analysed through a temporal cross correlation method, has found that surface pressure fluctuations have the highest correlation with upstream eddies. When implementing the finlets, results indicated a reduction in correlation at regions far away from the surface of the aerofoil, leaving behind an increase in the near wall correlation. This phenomenon is likely due to the breaking up of the large scale eddies down to smaller ones when passing between the finlets.

Based on what is known, prospective methods lie ahead in studying the near wall TBL structures, with strict correlation studies with the outer boundary layer dynamics. In the long term, this should lay the groundwork for exploring means to control the TBL through the breaking down of turbulent eddies from the upstream regions through to the trailing edge, in a goal to fine tune a passive device to reduce noise within a particular band. In addition, knowledge of the exact TBL structures, in near and outer wall regions, pre- and post-surface treatment, will shed light on numerical methods which can be implemented in a specific finlet design task.

2. WIND TUNNEL FACILITY, DATA ACQUISITION, TEST PARAMETERS, BASELINE DEFINITION

Far field noise measurements were conducted in the anechoic chamber at Brunel University. The anechoic chamber is fitted with an open loop open jet nozzle measuring 100mm in height, and 300mm in width. This wind tunnel is characterised by a freestream turbulence intensity of 0.1-0.2%, and a maximum jet velocity of 80m/s. The open jet noise characteristics of this wind tunnel have been validated by three case studies, all of which demonstrate a very low background noise relative to noise radiated from the test aerofoil (Vathylakis, Chong, & Kim, 2014). Far field noise measurements were taken using a polar array of eight microphones at a 1.0m radius each, situated at θ = 50°, 60°, 70°, 80°, 90°, 100°, 110°, 120° from the trailing edge respectively, with the aerofoil itself clamped between two vertical sideplates extending from the nozzle. The noise data was acquired at a sampling frequency of 40kHz for 10s by a 16-bit DAC from National Instruments. The Power Spectral Density of 1Hz Bandwidth and frequency resolution of 40kHz was generated using a 1024 point Fast Fourier Transform within MATLAB. The data is processed as $W = \frac{2\pi r}{\rho c}\int_{\theta_1}^{\theta_n} p_F$ where W is the sound power level, ρ is the medium density, c is the speed of sound in the given density, r is the observer distance, p_F is the acoustic pressure level at a given frequency interval, integrated across all microphone angles where $50 \leq \theta \leq 120$. The data is converted back to decibels by

$$PWL = 10\log\left(\frac{W}{W_{ref}}\right) \text{ where } W_{ref} = 10^{-12}W$$

Equation 1 PWL (Sound Power Level) definition

OAPWL (Overall sound power level) is derived by taking the integral of the power level spectrum. To obtain a greater sensitivity to changes in noise emission/reduction, the spectra are integrated between 1000-16000Hz. The OAPWL values were determined using the following method;

$$OAPWL = 10log_{10}\left(\frac{\int w(f)df}{W_{ref}}\right)$$

Equation 2 OAPWL (Overall Sound Power Level) definition

and ΔOAPWL is computed by taking the OAPWL of a given case and subtracting the dB values of the respective baseline case from it. Therefore a negative value of ΔOAPWL denotes noise reduction, while a positive one denotes noise increase.

In setting up the test aerofoil, a forced boundary layer transition was promoted using pieces of turbulator tape placed on the suction and pressure side of the aerofoil. This removes the laminar instability tonal noise as seen in *Figure 1* at ~2kHz and ~3.5kHz for 30 and 45m/s respectively. The

laminar instability noise is quite dominant in this aerofoil, therefore implementing a forced transition method ensures that the results obtained are using a consistent turbulent boundary layer under controlled conditions. The setup comes with a trade-off as zig-zag tips of the trip tape generating a visible peak at 8kHz and 15kHz for U=30 and 45m/s respectively at AOA=-10°, seen in *Figure 1* on the black line spectra.

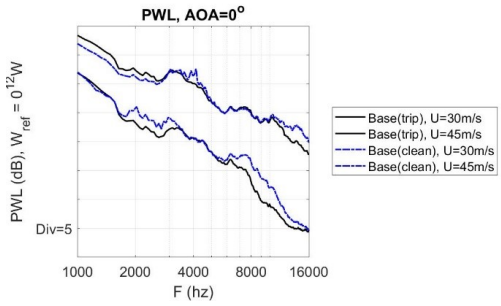

Figure 1 PWL, forced transition dependency, AOA=0° at U=30, 45m/s.

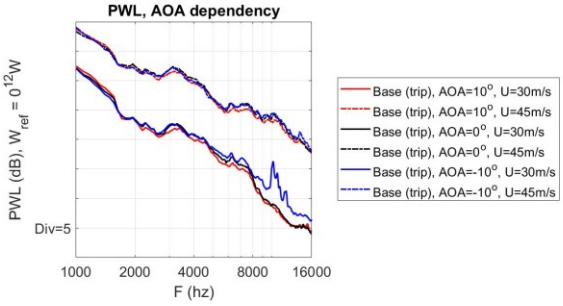

Figure 2 PWL, baseline AOA dependency

To further characterise the aerofoil, it is important to understand how the spectrum is expected to change with varying AOA, as shown in Figure 2. Under tripped conditions the spectra between AOA (geometric) = 10°, 0°, -10° shows a crossover between 2kHz and 4kHz, but this crossover is minimal. This may suggest that the range of effective AOA is small across the range of geometrical AOA tested in the current study.

By acquiring PWL data from a range of velocities U = 20, 30, 40, 50, 60m/s, any anomalies or unaccounted for phenomena can be observed. Apart from the aforementioned trip tape tonal peak visible at 30 and 40m/s for AOA=-10° at 8kHz and 16kHz respectively, the progression between velocities appears to be predictable. Taking the OAPWL values of each velocity spectrum from Figure 3, the obtained OAPWL values can be scaled against the U power law in Figure 4. Seeing as both curves are near parallel, one could confirm that the trailing edge noise is being radiated out in a dipole source manner. In one observation, it is worth noting that despite a large change in AOA up to ±10°, the spectrum does not change significantly, even though the boundary layer is expected to vary significantly at such angle deviations. Further boundary layer measurements will be required to explore the matter.

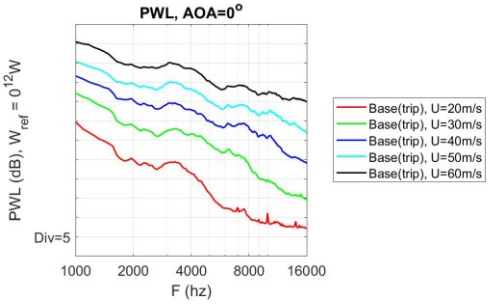

Figure 3 PWL, U dependency, AOA=0° at U=20, 30, 40, 50, 60m/s.

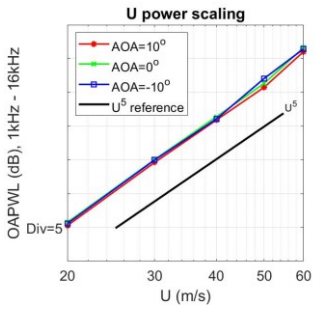

Figure 4 U power scaling, showing TE noise as dipole noise source

In order to confirm the noise reduction characteristics of finlets, a set of parameters described in Figure 5 were outlined in Table 1 with the following ratios of finlet height, and spacing, relative to a unit finlet thickness. The test program seeks to test all the various combinations of finlet height and spacing for the suction side only, and pressure side only as stated in Table 1, to observe the individual perceived reductions in OAPWL, and ΔOAPWL in relation to the baseline tripped aerofoil. Each finlet parameter configuration is tested at U=30m/s, and 45m/s, at AOA (geometric) = 10°, 0°, -10°.

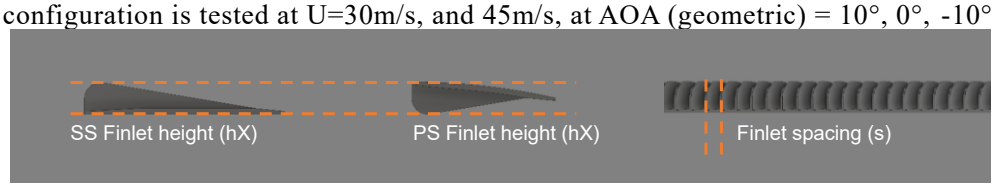

Figure 5 Finlet parameters described

Finlet height (hX)	hA < hB < hC < hD < hE
Finlet spacing (sX)	sA < sB < sC <sD

Table 1 Finlet parameters as ratios of unit thickness

3. SPACING-HEIGHT MATRICES, RESULTS AND OBSERVATIONS

To fulfil the aim of the current study into finlets, a series of test were conducted in combining the parameters outlined in Table 1. There is a separate case-set for AOA (geometric) = 10°, 0°, -10° at U=30m/s and AOA (geometric) = 10°, 0°, -10° at U=45m/s for pressure side of the aerofoil. The tested configurations are visible along the x-axis on the left-side absolute OAPWL plot, using spacing as an intermittent independent variable, and finlet height as the dependent. This way, the overall noise reduction trends can be visualised as a function of finlet height and spacing.

By observing the data ΔOAPWL surface plots, we can see an increase in performance with increasing finlet height, and reduction in finlet spacing. It is evident that the finlet performance decreases with high spacing and low height, as it would be exposing more of the trailing edge, now with additional bluntness. Where the finlets really do perform exceptionally is at high angles of attack. Based on the data, the additional height of the finlet does not add any detriment to the acoustic performance at near-zero AOA, but does add a considerable advantage at AOA=±10°.

With regards to the finlet parameters, spacing becomes the dominant factor, a trend which is confirmed by the works of (Clark, et al., 2015) and (Millican, 2017). By analysing the trend in absolute OAPWL, more closely packed finlets show greater increased in performance for every additional percent in added height. This however does not hold for more widely spaced finlets. What becomes curious with the suction side finlet performance in Figure 6 and Figure 7, is the relationship between sA and sB finlets. In both 30 and 45m/s cases, we see that the sB finlet shows a gradual performance increase with finlet height, where with sA the performance remains relatively unchanged up to and including sC. at hD, the sA finlets show an abrupt increase in performance. When observing data from the pressure side finlets, performance changes are more gradual across all spacings with the sA finlet performance scaling well with increasing height.

3.1 Finlet suction/pressure side only, U=30m/s, U=45m/s

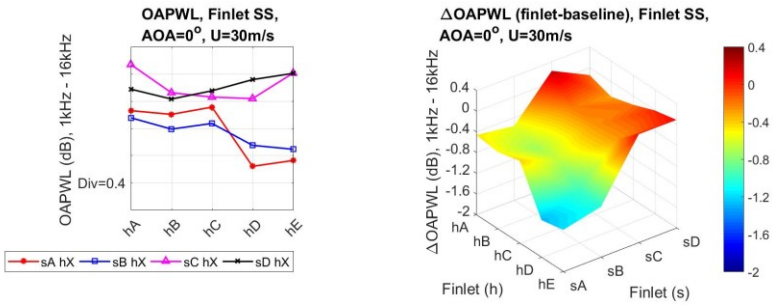

Figure 6 Finlet SS, OAPWL plot, ΔOAPWL surfplot, U=30m/s, AOA=0°

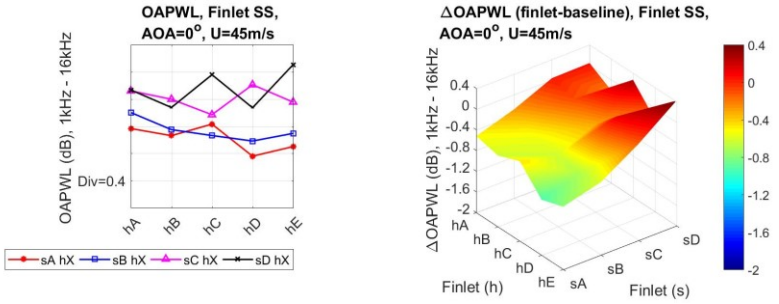

Figure 7 Finlet SS, OAPWL plot, ΔOAPWL surfplot, U=45m/s, AOA=0°

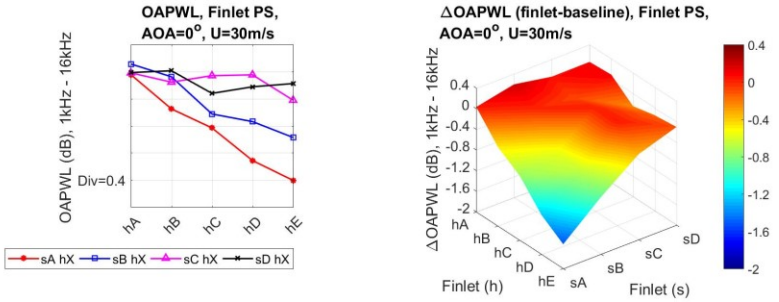

Figure 8 Finlet PS, OAPWL plot, ΔOAPWL surfplot, U=30m/s, AOA=0°

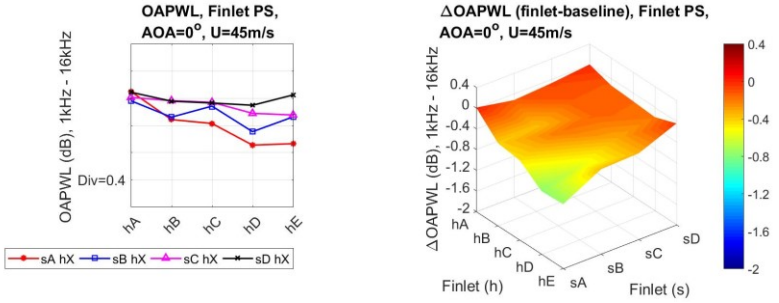

Figure 9 Finlet PS, OAPWL plot, ΔOAPWL surfplot, U=45m/s, AOA=0°

3.2 Finlet suction and pressure side combination

Figure 10 show the PWL spectra for finlets at suction and pressure sides when the same finlet configurations sA and hE are installed respectively. PWL produced by the untreated aerofoil is also included for comparison. Both cases exhibit good level of broadband noise reduction, but the surface add-on treatment on the pressure side seems to generate larger level of noise reduction than the suction side. This could be due to the finlet being more optimised to the TBL at the pressure side than the suction side. To understand more about the relationship between finlet configuration effects on the TBL, further testing and examination will be required. Secondly, is that in combination, the reduction performance is significantly augmented in the broadband spectrum, being able to offer reductions from 2kHz and upwards, while tracking the jet noise very closely offering reductions up to 7dB PWL.

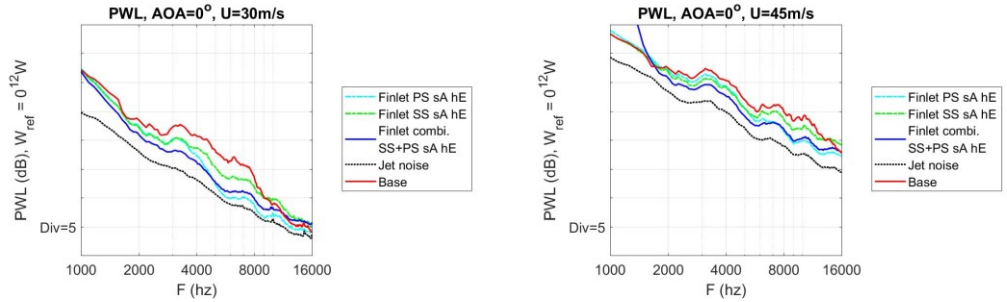

Figure 10 PWL comparison, baseline, finlet SS and PS, jet noise, AOA=0°, U=30m/s, 45m/s

To supplement the conclusion of improved finlet performance in relation to a baseline at high AOA, Figure 11 shows that between finlet-only configurations, performance is improves with increasing AOA. This is demonstrated by the red curves for AOA=10°, with noise emissions rising for AOA=0° and AOA=-10° respectively. Interestingly, the greater sensitivity of TE noise radiation with respect to the AOA, as exhibited by aerofoil with finlet treatment in Figure 11, is markedly different with the untreated, baseline aerofoil shown in Figure 2. This demonstrates that the finlet has disrupted the development of turbulent boundary layer far greater than the variation in pressure gradient. In a previous observation, it was stated that the main performance altering factor in finlets is the spacing parameter, and not so much the height. This would point into the direction that finlets exploit a boundary layer structure, whose prominence is characterised by a spanwise correlation length scale.

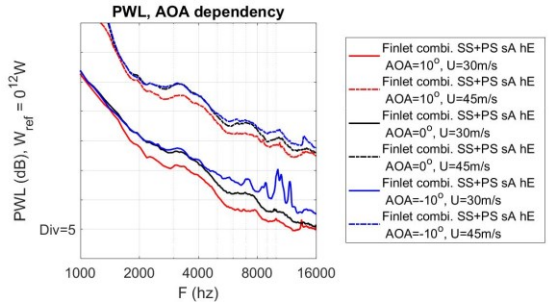

Figure 11 PWL, finlet SS+PS combi. AOA dependency

To model noise emissions of aerofoils under various configurations, a number of numerical models were devised over the years in the field of aeroacoustics. One of the better known methods was done by Amiet, which requires knowledge of the wall pressure spectrum near the trailing edge. The model itself does contain some inherent limitations, the first being the aerofoil is assumed to be a straight infinite flat plate extended into the upstream or downstream direction for leading and trailing edge noise respectively. The geometric effects of an aerofoil such as its shape, camber, thickness, trailing edge thickness is not considered, but rather the local wall pressure data used in the model. The far field acoustic spectrum S_{pp} can be predicted by Amiet's model from:

$$S_{pp}(X,\omega) = \left(\frac{sin\theta}{2\pi r}\right)^2 (kC)^2 \frac{d}{2} |\mathcal{L}|^2 \ell(\omega) \phi_{pp}(\omega), where$$

Equation 3 Amiet TE noise model

$X = (x_1, x_2, x_3)$ is the observer position with the origin located at centre-span on the trailing edge, $\left(\frac{sin\theta}{2\pi r}\right)^2$ is the observer location relative to the origin, $(kC)^2$ where k is the acoustic wave number and C is the chord length, $\frac{d}{2}$ is the foil semi span, $\mathcal{L}$ is the acoustic transfer function $\mathcal{L} = \mathcal{L}_1 + \mathcal{L}_2$ where $\mathcal{L}_1$ being the transfer function of the trailing edge, and $\mathcal{L}_2$ the back-scattering leading edge correction done by (Roger & Moreau, 2005), $\phi_{pp}(\omega)$ is the wall pressure power spectral density, $\ell(\omega)$ is the spanwise correlation length, The spanwise length correlation $\ell(\omega)$ is brought by the Corcos model (Corcos, 1967), same as in the Modified Howe model as $\ell(\omega) = \frac{U_c}{\gamma\omega}$ where U_c is the convective velocity, γ is a variable constant, and ω is a specified angular frequency.

In the works of (Clark, et al., 2015), (Millican, 2017), and (Afshari, Szoke, Denghan, & Azarpeyvand, 2016), a common hypothesis is upheld, where the performance of the finlet is mainly characterised by a combination of shifting the large turbulent structures away from the trailing edge, and the reduction of the spanwise coherence. In relation to the Amiet model presented in Equation 3, this would be seen in the reduction of the spanwise correlation $\ell(\omega)$, brought by the Corcos model (Corcos, 1967). The second parameter is the reduction of surface pressure fluctuations near the trailing edge as described by (Afshari, Szoke, Denghan, & Azarpeyvand, 2016) and (Bodling & Sharma, 2018) which would be impacting on the $\phi_{pp}(\omega)$ parameter of the model.

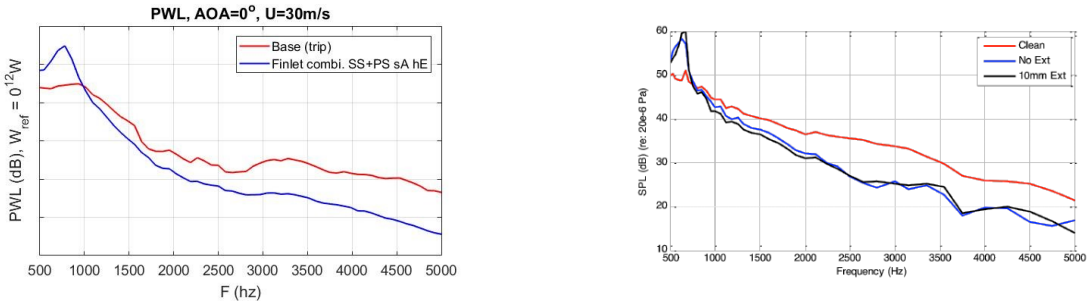

Figure 12 Comparison between spectra from current study (left) and study conducted by (Clark, et al., 2015) (right).

In the absence of detailed flow measurement in the current study, the results obtained in this study are found to be in line to that of (Clark, et al., 2015), as shown in Figure 12. The results obtained here confirm some of the basic trends observable in finlet configuration geometry with regards to their aeroacoustics performance at varying speeds and AOA.

4. CONCLUSIONS AND FURTHER WORK

To conclude this short study into the aeroacoustic performance trends of finlets, several outcomes become clear; Finlet performance improves with increasing finlet height, and decreasing spacing. Individually, finlets are able to produce up to 2dB broadband noise reduction with no trade-off. A combination of suction side and pressure side finlets offers excellent reductions up to 7dB, and can offer more once optimised. The main parameter for improved performance of finlets is the spacing rather than the height. Finlet height does not offer any significant impact on the performance if the spacing is not optimal. With regards to AOA performance, the established trend for optimal finlet parameters remained consistent for all AOA, offering greater reductions at high angles, which is a good sign for practical applications in wind turbine blades.

Further work based on this study would include the boundary layer measurements through the use of multi-hotwire and wall pressure transducers. This is required to understand how finlets affect the aforementioned spanwise correlation $\ell(\omega)$, and surface pressure fluctuation variables $\phi_{pp}(\omega)$. The main focus would be to correlate the near wall changes in the boundary layer to the simultaneous changes in the far-field measurements. This would serve well in developing a numerical solution/extension to an existing semi-empirical aerofoil noise model to get a closer look into the full potential of optimised finlet reduction performance.

Exploring the TBL eddy structure in the near wall and outer wall region in details is imperative, especially that a non-linear effect for the boundary layer contribution to the noise radiation subjected to finlet treatment has been observed. Having the ability to use correlation studies to characterise the use of finlets in breaking down large TBL structures into smaller ones could shed light on the future development of multi-stage noise reduction devices. These devices would focus on the upstream flow to disrupt turbulence inducing phenomena, paired with methods of sheltering the trailing edge from high energy turbulent structures.

REFERENCES

1. Afshari, A., Szoke, M., Denghan, A. A., & Azarpeyvand, M. (2016). Trailing edge noise reduction Using Novel Surface Treatments. *AIAA 2016-2834*.
2. Arnold, B., Lutz, T., & Kramer, E. (2018). Design of a boundary-layer suction system for turbulent trailing edge noise reduction of wind turbines. *Renewable Energy, 123*.
3. Bodling, A., & Sharma, A. (2018). Numerical Investigation of Low-Noise Airfoils Inspired by the Down Coat of Owls. *AIAA 2018-3925*.
4. Brooks, T., Pope, D., & Marcolini, M. (1989). *Airfoil self-noise and prediction.* NASA.
5. Chong, T. P., & Joseph, P. (2012). “Ladder” structure in tonal noise generated by laminar flow around an aerofoil. *The Journal of the Acoustical Society of America, 131*.
6. Clark, I., Alexander, N., Devenport, W., Stewart Glegg, J. J., Peake, N., & Daly, C. (2015). Bio-Inspired Trailing Edge Noise Control. *AIAA 2015-2365*.
7. Corcos, G. M. (1967). The resolution of turbulent pressures at the wall of a boundary layer. *Journal of Sound and Vibration, 6*.
8. Fischer, G. R., Kipouros, T., & Savill, A. M. (2014). Multi-objective optimisation of horizontal axis wind turbine structure and energy production using aerofoil and blade properties as design variables. *Renewable Energy, 62*.
9. Gao, L., Zhang, H., Liu, Y., & Han, S. (2015). Effects of vortex generators on a blunt trailing-edge airfoil for wind. *Renewable Energy, 76*.
10. Gruber, M., Joseph, P., & Chong, T. (2010). Experimental investigation of airfoil self noise and tubulent wake reduction by the use of trailing edge serrations. *16th AIAA/CEAS Aeroacoustics Conference.*
11. Herr, M., Bahr, C., & Kamruzzaman, M. (2014). Workshop Category 1: Trailing-Edge Noise. *Third Workshop on Benchmark Problems for Airframe Noise Computations (BANC-III)*.
12. Kingan, M. J., & Pearse, J. R. (2009). Laminar boundary layer instability noise produced by an aerofoil. *Journal of Sound and Vibration, 322*, 808-828.
13. Küçükosman, Y., Christophe, J., & Schram, C. (2018). Trailing edge noise prediction based on wall pressure spectrum models for NACA0012 airfoil. *Journal of Wind Engineering & Industrial Aerodynamics, 175*, 305-316.
14. Lighthill, M. (1954). *On sound generated aerodynamically II. Turbulence as a source of sound.* Royal Society.
15. Mathew, J., Singh, A., Madsen, J., & Leon, C. (2016). Serration Design Methodology for Wind Turbine

Noise Reduction. *Journal of Physics: Conference Series, 753*.
16. Millican, A. J. (2017). *Bio-Inspired Trailing Edge Noise Control: Acoustic and Flow Measurement.* Virginia Polytechnic Institute and State University.
17. Moreau, D., Brooks, L., & Doolan, C. (2011). Flat plate self noise reduction at low-to-moderate Reynolds number with trailing edge serrations. *Proceedings on the Annual Conference on the Australian Acoustical Society.*
18. Office of Energy Efficiency & Renewable Energy. (2017). *Advantages and Challenges of Wind Energy*. Retrieved from Office of Energy Efficiency & Renewable Energy: https://www.energy.gov/eere/wind/advantages-and-challenges-wind-energy
19. Roger, M., & Moreau, S. (2005). Back-Scattering correction and further extenrions of Amiet's trailing-edge noise model. *Journal of Sound and Vibration, 286*.
20. Sapkale, S. L., Sucheendran, M. M., Gupta, S. S., & Kanade, S. V. (2018). Vibroacoustic study of a point-constrained in a duct. *Journal of Sound and Vibration, 420*.
21. The Shift Project Data Portal. (2017). *Breakdown of Electricity Generation by Energy Source*. Retrieved from The Shift Project Data Portal: http://www.tsp-data-portal.org/Breakdown-of-Electricity-Generation-by-Energy-Source#tspQvChart
22. U.S. Energy Information Administration. (2017). *International Energy Outlook 2017*. Retrieved from U.S. Energy Information Administration: https://www.eia.gov/outlooks/ieo/
23. Van Der Velden, W., Romani, G., & D.Casalino. (2018). Wind Turbine Noise Prediction. *4th Wind and Drivetrain Conference.* Hamburg, Germany.
24. Vathylakis, A., Chong, T. P., & Kim, J. H. (2014). Design of a low-noise aeroacoustic wind tunnel facility at Brunel University. *AIAA , 2014-3288*.
25. Vestas Wind Systems A/S. (2017). *V150-4.2MW Technical Specifications*. Retrieved from Vestas Wind Systems A/S: https://www.vestas.com/en/products/turbines/v150-4_2_mw#!technical-specifications
26. World Energy Council. (2016). *World Energy Resources 2016*. Retrieved from World Energy Council: https://www.worldenergy.org/data/resources/
27. Wu, L., Jing, X., & Sun, X. (2017). Prediction of vortex-shedding noise from the blunt trailing edge of a flat plate. *Journal of Sound and Vibration, 408*.